

# PHOTOCATALYTIC PROPERTIES OF HEXAGONAL WO<sub>3</sub> NANOWIRES DECORATED WITH GOLD NANOPARTICLES

Tamás FIRKALA,<sup>a</sup> Orsolya KÉRI,<sup>a</sup> Fanni GÁBER,<sup>a</sup> Lenke KÓCS,<sup>b</sup> Zoltán HÓRVÖLGYI,<sup>b</sup> Dávidné NAGY,<sup>c</sup> Maria ZAHARESCU<sup>d</sup> and Imre Miklós SZILÁGYI<sup>a,e\*</sup>

<sup>a</sup>Department of Inorganic and Analytical Chemistry, Budapest University of Technology and Economics, Műegyetem rakpart 4., Budapest 1111, Hungary

<sup>b</sup>Department of Physical Chemistry and Materials Science, Budapest University of Technology and Economics, H-1521 Budapest, Budafoki út 6-8, Hungary

<sup>c</sup>Institute for Materials and Processes, School of Engineering, The University of Edinburgh, The King's Buildings, Mayfield Road, Edinburgh, EH9 3JL, United Kingdom

<sup>d</sup>“Ilie Murgulescu” Institute of Physical Chemistry, Romanian Academy, 202 Splaiul Independenței, 060021 Bucharest, Romania

<sup>e</sup>MTA-BME Research Group of Technical Analytical, Szent Gellért tér 4., Budapest, H-1111, Hungary

\* Corresponding author: imre.szilagyi@mail.bme.hu

*Received October 3, 2016*

Hexagonal WO<sub>3</sub> nanowires (h-WO<sub>3</sub> NWs) (5-10 nm thick, 10 μm long) were prepared with microwave assisted hydrothermal synthesis using aqueous Na<sub>2</sub>WO<sub>4</sub>, (NH<sub>4</sub>)<sub>2</sub>SO<sub>4</sub> and HCl. They were decorated with 5-10 nm gold nanoparticles, which were deposited by impregnation with HAuCl<sub>4</sub> and NH<sub>4</sub>OH solutions and consecutive annealing at 350 °C. XRD, TEM, EDX and diffuse reflectance UV-Vis were applied for characterization, which demonstrated the presence of gold nanoparticles immobilized on the h-WO<sub>3</sub> NWs. The photocatalytic activity of the as-prepared nanomaterials was tested in decomposing aqueous methyl orange. Without the heat treatment at 350 °C, the h-WO<sub>3</sub>-Au sample did not have an increased activity, compared to bare h-WO<sub>3</sub> nanowires. However, after annealing the formation of gold nanoparticles was more intense, and thus the photocatalytic performance of the h-WO<sub>3</sub>-Au sample grew 2.5 times higher, due to suppressed electron-hole recombination.

## INTRODUCTION

Tungsten oxide (WO<sub>3</sub>) is an n-type semiconductor material and its importance was revealed in several fields, *e.g.* catalysis, photocatalysis, gas sensing, electrochromic devices, etc.<sup>1-8</sup>. WO<sub>3</sub> has

several polymorphs with different crystalline arrangements, the monoclinic/triclinic/orthorhombic/tetragonal, the hexagonal and the cubic. Please note that the triclinic, monoclinic, orthorhombic and tetragonal  $\text{WO}_3$  phases have basically the same chessboard-like arrangement of  $\text{WO}_6$  octahedra, and they differ only in the displacement of W atoms from the center of  $\text{WO}_6$  octahedra<sup>9-14</sup>. Except for electrochromic applications, mostly monoclinic  $\text{WO}_3$  was tested in the applications, and there are only few studies about the properties of the hexagonal  $\text{WO}_3$  in catalysis<sup>15</sup>, photocatalysis<sup>16</sup> and gas sensing<sup>17-21</sup>.

In the last decades various methods were developed to synthesize of tungsten oxide nanostructures, including sol-gel, electrospinning, gas phase deposition methods, hydrothermal synthesis, thermal decomposition of precursors, etc<sup>22-30</sup>. However there is continuously a high demand for new synthesis methods due to several reasons. The general requirements, for instance, of green chemistry require more and more environmental friendly technologies taking emphasize on aqueous phase preparations, good atom efficiency using renewable feedstocks, etc<sup>31-32</sup>.

Liquid phase microwave synthesis methods are important segments of green chemistry technology<sup>33-34</sup>. It is a very effective way to improve already well-functioning laboratory scale reactions, but it is a promising direction for larger scale industrial production also<sup>35</sup>. Microwave heating methods have several advantages, compared to conventional solvent heating processes. Lower reaction temperatures, for instance, considerably shorter process times, higher yields, purer reaction products, higher level reaction reproducibility and temperature distribution homogeneity can be achieved much more easily<sup>36</sup>.

About the microwave assisted preparation of  $\text{WO}_3$ , there were only few studies conducted, and these produced mostly monoclinic  $\text{WO}_3$ <sup>37-41</sup>. Recently, a novel method was described for the preparation of  $\text{WO}_3$  nanowires in hexagonal crystal form with microwave assisted hydrothermal reaction<sup>42</sup>. The process resulted in unique hexagonal (h)  $\text{WO}_3$  nanowires (NWs) with 10 nm average diameter and remarkable increase in BET surface, which are promising parameters for various applications.

Therefore our goal was to study the photocatalytic potential of these hexagonal  $\text{WO}_3$  nanowires, and if possible increase it even further. Noble metals are traditionally applied materials for catalytic applications<sup>43-45</sup>. Several  $\text{WO}_3$ /noble metal nanostructures were also investigated in various catalytic test systems and the increased activity was connected to the presence of noble metals in practically every case<sup>46-47</sup>. Hence we aimed to decorate the h- $\text{WO}_3$  NWs with Au nanoparticles to achieve increased photocatalytic activity.

Accordingly, in this study, h- $\text{WO}_3$  nanowires were obtained with microwave assisted hydrothermal synthesis using aqueous solution of  $\text{Na}_2\text{WO}_4$ ,  $(\text{NH}_4)_2\text{SO}_4$  and HCl. The nanowires were decorated with gold nanoparticles by impregnation with  $\text{HAuCl}_4$  and  $\text{NH}_4\text{OH}$  solutions and consecutive annealing at 350 °C. X-ray diffraction (XRD), transmission electron microscopy (TEM), energy dispersive X-ray analysis (EDX) and diffuse reflectance UV-Vis spectroscopy were applied for

nanomaterials characterization. The photocatalytic activity of the as-prepared nanomaterials was tested in decomposing methyl orange in its aqueous solution.

## **EXPERIMENTAL**

### **Sample preparation**

For the preparation of h-WO<sub>3</sub> nanowires (NWs) a microwave-assisted hydrothermal synthesis method was applied. At first, 1.5 g Na<sub>2</sub>WO<sub>4</sub>·2H<sub>2</sub>O was dissolved in 33.75 mL H<sub>2</sub>O, then under stirring 3.75 mL 3 M HCl was added dropwise and finally 22.5 mL 0.5 M (NH<sub>4</sub>)<sub>2</sub>SO<sub>4</sub> was introduced. The as-prepared solution was heated to 160 °C in 20 min, then kept at 160 °C for 3 hours in a Synthos 3000 Anton Paar microwave hydrothermal reactor. The solid reaction product was centrifuged, then washed two times with water, once with ethanol, and again two times with water. In each washing step, 45 mL solvent was poured over the crystals, the dispersion was stirred for 1 min, and centrifuged for 5 min at 6000 1/min. Finally, the as-prepared h-WO<sub>3</sub> NWs were dried at 80 °C for 12 hours. The yield was 64 %.

For gold nanoparticle deposition onto h-WO<sub>3</sub> NWs, 100 mg h-WO<sub>3</sub> NWs were suspended in 60 mL 3.1\*10<sup>-4</sup> M tetrachloroauric acid (HAuCl<sub>4</sub>) solution and pH of the solution was set to 7 by adding 4 M aqueous solution of NH<sub>4</sub>OH dropwise. After 75 min vigorous stirring at pH 7, the suspension was decanted, washed with de-ionized water and centrifuged 3 times. The product was dried 20 h at 60 °C, and was named h-WO<sub>3</sub>-Au-1.

Then this sample was heated to 350 °C in 30 min and kept there for 1 h in air in a Nabertherm Controller B170 furnace, washed with de-ionized water, centrifuged 3 times at room temperature and dried at 60 °C for 3 h. This second sample was named h-WO<sub>3</sub>-Au-2. The main difference between h-WO<sub>3</sub>-Au-1 and h-WO<sub>3</sub>-Au-2 was the annealing at 350 °C in the case of h-WO<sub>3</sub>-Au-2.

### **Characterization methods**

TEM and HR-TEM images were recorded on a FEI Morgagni 268b TEM instrument operated at 100 keV.

XRD patterns were measured by a PANalytical X'pert Pro MPD X-ray diffractometer using Cu K<sub>α</sub> radiation.

EDX data were obtained by a JEOL JSM-5500LV scanning electron microscope equipped with an iXRF EDX detector.

UV-VIS reflection spectra about the powder samples were measured by an Avantes 2048 UV-Vis spectrometer with 45° angle between the sample surface and the optical cable. The band gap

energy with  $\pm 0.05$  eV uncertainty was calculated by creating a Tauc plot and extrapolating the tangent line to zero.

## Photocatalysis

The photocatalytic activity of the nanomaterials was tested in photo-bleaching reaction of aqueous methyl-orange (MO) solution. The powder samples (3 mg) were immersed into 3 mL 0.0133 mg/mL methyl orange solution in quartz cuvettes. The cuvettes were placed between two parallel 18 W Osram black lights; the distance between the lamps was 20 cm. To reach adsorption equilibrium between the powders and the dye prior to UV irradiation, the samples were stirred in dark for 20-120 minutes. After turning on the UV lamps, UV-VIS monitoring of the reaction was carried out with a Jasco V-550 UV-VIS spectrometer using the cuvettes where the reactions took place, and the conversion was checked in every 30 minutes. The absorption (proportional to concentration) decrease of methyl orange was measured at its absorption maximum (464 nm). To have a correct comparison for each sample, relative absorbance  $A/A_0$  values were calculated, where  $A_0$  is the absorbance at the beginning of the photocatalysis reaction and  $A$  is the actual absorbance at the certain measurement point.

## RESULT AND DISCUSSION

### Formation of Au decorated h-WO<sub>3</sub> nanowires

Figure 1 shows the XRD patterns of h-WO<sub>3</sub> NW, h-WO<sub>3</sub>-Au-1 and h-WO<sub>3</sub>-Au-2 samples. The synthesis of the h-WO<sub>3</sub> NW sample was successful, since it contained only hexagonal tungsten oxide (ICDD 85-2460) without the presence of any other phases. When Au was deposited on the h-WO<sub>3</sub> NWs, the presence of metallic gold (ICDD 04-0784) was clearly shown by the peak at 38° (see the inset of Fig. 1). This peak was more intense in the case of the h-WO<sub>3</sub>-Au-2 sample, which supports the importance of annealing at 350 °C for the formation of Au nanoparticles.

TEM images demonstrate that h-WO<sub>3</sub> was synthesized in the form of nanowires, which were ca. 10 nm in diameter and 10 μm in length (Fig. 2a). High resolution (HR-TEM) images (Fig. 2b) confirmed that the nanowires were single crystalline. After the reaction with the HAuCl<sub>4</sub> solution and annealing at 350 °C (h-WO<sub>3</sub>-Au-2), 5-10 nm gold nanoparticles were generated on the surface of h-WO<sub>3</sub> NWs (Fig. 2c).

EDX results revealed that h-WO<sub>3</sub> NWs were composed of only W and O, and they had no contamination originating from the precursors; thus, the conditions were adequate for the microwave hydrothermal reaction and the subsequent washing steps. EDX also confirmed the presence of Au on h-WO<sub>3</sub>-Au-1 and h-WO<sub>3</sub>-Au-2. The gold content on these samples was ca. 0.1 m/m%.

The h-WO<sub>3</sub> NW sample was yellow and its absorption edge was at about 475 nm (Fig. 3a). From the Tauc plot (see inset on Fig. 3) the band gap of h-WO<sub>3</sub> NW was calculated to be  $2.75 \pm 0.05$  eV, which is a typical value for h-WO<sub>3</sub> nanocatalysts<sup>48-50</sup>. When h-WO<sub>3</sub> NWs were impregnated with the HAuCl<sub>4</sub> and NH<sub>4</sub>OH solutions (h-WO<sub>3</sub>-Au-1), a small peak appeared at 550 nm (Fig. 3b). This showed that already at this stage some Au nanoparticles formed. After annealing at 350 °C the intensity of this peak increased significantly, confirming that the formation of Au nanoparticles was more intense (Fig. 3c).

### Photocatalysis

At first, as a reference, the decomposition of methyl orange was monitored without the presence of photocatalyst (photolysis). After 120 min reaction time the relative absorbance of methyl orange and thus its concentration proportional to that decreased only by 2 % (Fig. 4). When h-WO<sub>3</sub> NWs were put into the methyl orange solution, the concentration of the solution decreased by 11 % at the end of the reaction, showing clearly the photocatalytic activity of the sample. When the h-WO<sub>3</sub> NWs were impregnated with the HAuCl<sub>4</sub> and NH<sub>4</sub>OH solutions but the annealing step at 350 °C was omitted (h-WO<sub>3</sub>-Au-1), the photocatalytic activity did not change significantly, compared to the bare h-WO<sub>3</sub> NWs. In contrast, when the formation of Au nanoparticles was more intense after annealing at 350 °C (h-WO<sub>3</sub>-Au-2), the photocatalytic activity also increased a great deal. After 2 h reaction time, when the h-WO<sub>3</sub>-Au-2 was used as photocatalyst, the concentration of methyl orange decreased by 25 %, which is ca. 2.5 times better activity compared to bare h-WO<sub>3</sub> NWs and the h-WO<sub>3</sub>-Au-1 sample. The results showed that without the annealing at 350 °C, the treatment with HAuCl<sub>4</sub> solution is ineffective for obtaining Au nanoparticle decorated WO<sub>3</sub> photocatalysts with better photocatalytic activity.

The doping of h-WO<sub>3</sub> NWs with gold nanoparticles was effective in reaching higher photocatalytic activity, because an electron transfer can take place between the n-type semiconductor oxide h-WO<sub>3</sub> material and the Au nanoparticles. Au can easily accommodate electrons coming from the photo-generated electron-hole pairs in h-WO<sub>3</sub>. This way the recombination of electrons and holes is suppressed, which leads directly to a higher photocatalytic activity<sup>51-53</sup>.

### CONCLUSIONS

In this work WO<sub>3</sub> nanowires were synthesized with microwave assisted hydrothermal reaction in hexagonal crystal form. Gold nanoparticles were deposited onto the surface of nanowires using impregnation with HAuCl<sub>4</sub> and NH<sub>4</sub>OH solutions and consecutive annealing at 350 °C, aiming photocatalytic promoting effect. The photocatalytic activity of the samples was investigated in the photo-bleaching reaction of methyl-orange. Without the heat treatment at 350 °C, the h-WO<sub>3</sub>-Au-1

sample did not have an increased photocatalytic activity, compared to bare h-WO<sub>3</sub> nanowires. However, after annealing the formation of gold nanoparticles was more intense, and thus the photocatalytic performance of the h-WO<sub>3</sub>-Au-2 sample became 2.5 times higher. The reason for the higher photocatalytic efficiency was the transfer of photo-induced electrons from the h-WO<sub>3</sub> substrate to the Au nanoparticles, which decreased the electron-hole recombination. Our results support that gold doping is an effective way to enhance the photocatalytic activity of hexagonal WO<sub>3</sub>.

*Acknowledgments:* T. Firkala acknowledges a PhD Scholarship of Richter Gedeon Plc (Hungary). I. M. Szilágyi thanks for a János Bolyai Research Fellowship of the Hungarian Academy of Sciences. An OTKA-PD-109129 grant is acknowledged. The financial support of the National Development Agency (Hungarian-French Bilateral Co-operation, PHONOSEL, TÉT\_11-2-2012-0008) is gratefully acknowledged.

## REFERENCES

1. C. Hoang-Van and O. Zegaoui, *App. Catal. A*, **1997**, *164*, 91.
2. C. Hoang-Van and O. Zegaoui, *App. Catal. A*, **1995**, *130*, 89.
3. C. Hammond, J. Straus, M. Righettoni, S.E. Pratsinis and I. Hermans, *ACS Catal.*, **2013**, *3*, 321.
4. M. Qamar, M.A. Gondal and Z.H. Yamani, *Catal. Commun.*, **2010**, *11*, 768.
5. I.M. Szilágyi, E. Santala, M. Heikkilä, V. Pore, M. Kemell, G. Teucher, T. Firkala, E. Färm, T. Nikitin, L. Khriachtchev, M. Räsänen, M. Ritala and M. Leskelä, *Chem. Vapor Dep.*, **2013**, *19*, 149.
6. S. Santucci and W. Wlodarski, *J. Vac. Sci. Technol. A*, **1999**, *17*, 1873.
7. S.M. Kanan and C.P. Tripp, *Synthesis, Curr. Op. Sol. St. Mat. Sci.*, **2007**, *11*, 19.
8. S. Papaefthimiou, G. Leftheriotis and P. Yianoulis, *Electrochim. Acta*, **2001**, *46*, 2145.
9. I.M. Szilágyi, J. Madarász, G. Pokol, I. Sajó, P. Király, G. Tárkányi, A.L. Tóth, A. Szabó and K. Varga-Josepovits, *J. Therm. Anal. Calorim.*, **2009**, *98*, 707.
10. I.M. Szilágyi, J. Madarász, G. Pokol, F. Hange, G. Szalontai, K. Varga-Josepovits and A.L. Tóth, *J. Therm. Anal. Calorim.*, **2009**, *98*, 11.
11. R.J.D. Tilley, *Int. J. Refract. Met. Hard. Mater.*, **1995**, *13*, 93.
12. E. Lassner and W.D. Schubert, *Properties, Chemistry, Technology of the Elements, Alloys, and Chemical Compounds*, Kluwer Academic / Plenum Publishers, New York, 1999.
13. I.M. Szilágyi, J. Madarász, F. Hange and G. Pokol, *Solid State Ionics*, **2004**, *172*, 583.
14. C. Chacón, M. Rodríguez-Pérez, G. Oskam and G. Rodríguez-Gattorno, *J. Mater. Sci. Mater. Electron*, **2015**, *26*, 5526.

15. I.M. Szilágyi, B. Fórizs, O. Rosseler, Á. Szegedi, P. Németh, P. Király, G. Tárkányi, B. Vajna, K. Varga-Josepovits, K. László, A. L. Tóth, Péter Baranyai and M. Leskelä, *J. Catal.*, **2012**, *294*, 119.
16. T. Firkala, B. Fórizs, E. Drotár, A. Tompos, A.L. Tóth, K. Varga-Josepovits, K. László, M. Leskelä and I.M. Szilágyi, *Catal. Lett.*, **2014**, *144*, 831.
17. I.M. Szilágyi, S. Saukko, J. Mizsei, A.L. Tóth, J. Madarász and G. Pokol, *Solid State Sci.*, **2010**, *12*, 1857.
18. I.M. Szilágyi, L. Wang, P.I. Gouma, C. Balázsi, J. Madarász and G. Pokol, *Mater. Res. Bull.*, **2009**, *44*, 505.
19. I.M. Szilágyi, J. Madarász, G. Pokol, P. Király, G. Tárkányi, S. Saukko, J. Mizsei, A.L. Tóth, A. Szabó and K. Varga-Josepovits, *Chem. Mater.*, **2008**, *20*, 4116.
20. C. Balázsi, L. Wang, E.O. Zayim, I.M. Szilágyi, K. Sedlackova, J. Pfeifer, A.L. Tóth and P.I. Gouma, *J. Eur. Ceram. Soc.*, **2008**, *28*, 913.
21. I.M. Szilágyi, S. Saukko, J. Mizsei, P. Király, G. Tárkányi, A.L. Tóth, A. Szabó, K. Varga-Josepovits, J. Madarász and G. Pokol, *Mater. Sci. Forum*, **2008**, 589, 161.
22. H. Long, W. Zeng and H. Zhang, *J. Mater. Sci. Mater Electron*, **2015**, *26*, 4698.
23. I.M. Szilágyi, E. Santala, M. Heikkilä, M. Kemell, T. Nikitin, L. Khriachtchev, M. Räsänen, M. Ritala and M. Leskelä, *J. Therm. Anal. Calorim.*, **2011**, *105*, 73.
24. S. Chen, Y. Hu, X. Jiang, S. Meng and X. Fu, *Mater. Chem. Phys.*, **2015**, *149-150*, 512.
25. L Yin, D. Chen, H. Zhang, G. Shao, B. Fan, R. Zhang and G. Shao, *Mater. Chem. Phys.*, **2014**, *148*, 1099.
26. E. Luevano-Hipolito, A. Martínez-de la Cruz, E.Lopez-Cuellar, Q.L. Yu and H.J.H. Brouwers, *Mater. Chem. Phys.*, **2014**, *148*, 208.
27. Z. Gu, H. Li, T. Zhai, W. Yang, Y. Xia, Y. Ma and J. Yao, *J. Solid State Chem.*, **2007**, *180*, 98.
28. I.M. Szilágyi, J. Pfeifer, C. Balázsi, A.L. Tóth, K. Varga-Josepovits, J. Madarász and G. Pokol, *J. Therm. Anal. Calorim.*, **2008**, *94*, 499.
29. C.L. Dezelah IV, O.M. El-Kadri, I.M. Szilágyi, J.M. Campbell, K. Arstila, L. Niinistö and C.H. Winter, *J. Am. Chem. Soc.*, **2006**, *128*, 9638.
30. J.M. Ortega, A.I. Martinez, D.R. Acosta and C.R. Magana, *Sol. En. Mat. Sol. Cell.*, **2006**, *90*, 2471.
31. P.T. Anastas, J.C. Warner, *Green Chemistry: Theory and Practice*, Oxford University Press, New York, 1998.
32. P.T. Anastas and J.B. Zimmerman, *Env. Sci. Tech.*, **2003**, *37*, 94A.
33. M.B. Gawande, S.N. Shelke, R. Zboril and R.S. Varma, *Acc. Chem. Res.*, **2014**, *47*, 1338.
34. C.R. Strauss and R.S. Warma, *Microwav. Meth. Org. Synt.*, **2006**, *266*, 199
35. H.J. Kitchen, S.R. Vallance, J.L. Kennedy, N. Tapia-Ruiz, L. Carassiti, A. Harrison, A.G. Whittaker, T.D. Drysdale, S.W. Kingman and D.H. Gregory, *Chem. Rev.*, **2014**, *114*, 1170.

36. S. Shi and J.Y. Hwang, *J. Min. Mater. Char. Eng.*, **2003**, 2, 101.
37. Y. Li, X. Su, J. Jian and J. Wang, *Ceram. Int.*, **2010**, 36, 1917.
38. J. Pfeifer, E.G. Badaljan, P. Tekula-Buxbaum, K. Vadasdi, *J. Solid State Chem.* 105 (1993) 588.
39. J. Pfeifer, B.A. Kiss, P. Tekula-Buxbaum and K. Vadasdi, *Int. J. Refract. Met. Hard. Mater.*, **1993-1994**, 12, 27.
40. Y. Gui, J. Zhao, W. Wang, J. Tian and M. Zhao, *Mater. Lett.*, **2015**, 155, 4.
41. D.B. Hernandez-Uresti, D. Sánchez-Martínez, A. Martínez-de la Cruz, S. Sepúlveda-Guzmán and L.M. Torres-Martínez, *Ceram. Int.*, **2014**, 40, 4767.
42. Phuruangrat, D.J. Ham, S.J. Hong, S. Thongtem and J.S. Lee, *J. Mater. Chem.*, **2010**, 20, 1683.
43. B. Wen, J. Ma, C. Chen, W. Ma, H. Zhu and J. Zhao, *Sci. China Chem.*, **2011**, 54, 887.
44. M.S. Hegde, G. Madras and K.C. Patil, *Acc. Chem. Res.*, **2009**, 42, 704.
45. W.T. Lu, J.C. Chen, J. Feng and J. Yu, *Rare Metal Mat. Eng.*, **2012**, 41, 184.
46. Z.-G. Zhao and M. Miyauchi, *Angew. Chem. Int. Ed.*, **2008**, 47, 7051.
47. E. Dvininov, U.A. Joshi, J.R. Darwent, J.B. Claridge, Z. Xu and M.J. Rosseinsky, *Chem. Commun.*, **2011**, 47, 881.
48. K.O. Iwu, A. Galeckas, P. Rauwel, A.Y. Kuznetsov and T. Norby, *J. Solid State Chem.*, **2012**, 185, 245.
49. K. Huang, Q. Zhang, F. Yang and D.Y. He, *Nano Res.*, **2010**, 3, 281.
50. J. Yu, L. Qi, B. Cheng and X. Zhao, *J. Hazard. Mater.*, **2008**, 160, 621.
51. L. Palmisano, V. Augugliaro, A. Sclafani and M. Schiavello, *J. Phys. Chem.*, **1988**, 92, 6710.
52. J.A. Navio, J.J. Testa, P. Djedjeian, J.R. Padron, D. Rodriguez and M.I. Litter, *Appl. Catal. A*, **1999**, 178, 191.
53. J.M. Hermann and J. Disdier, *P. Pichat, Chem. Phys. Lett.*, **1984**, 108, 618.

## Captions

Figure 1. XRD analysis of (a) h-WO<sub>3</sub> NW; (b) h-WO<sub>3</sub>-Au-1;(c) h-WO<sub>3</sub>-Au-2 samples

Figure 2. TEM images of (a-b) h-WO<sub>3</sub> NW; (c) h-WO<sub>3</sub>-Au-2 samples

Figure 3. Diffuse reflectance UV-VIS spectra of investigations of (a) h-WO<sub>3</sub> NW; (b) h-WO<sub>3</sub>-Au-1;(c) h-WO<sub>3</sub>-Au-2 samples

Figure 4. Degradation (absorption decrease at 464 nm) of methyl orange under UV illumination (a) without photocatalyst; and with (b) h-WO<sub>3</sub> NW; (c) h-WO<sub>3</sub>-Au-1; (d) h-WO<sub>3</sub>-Au-2 samples

## Figures

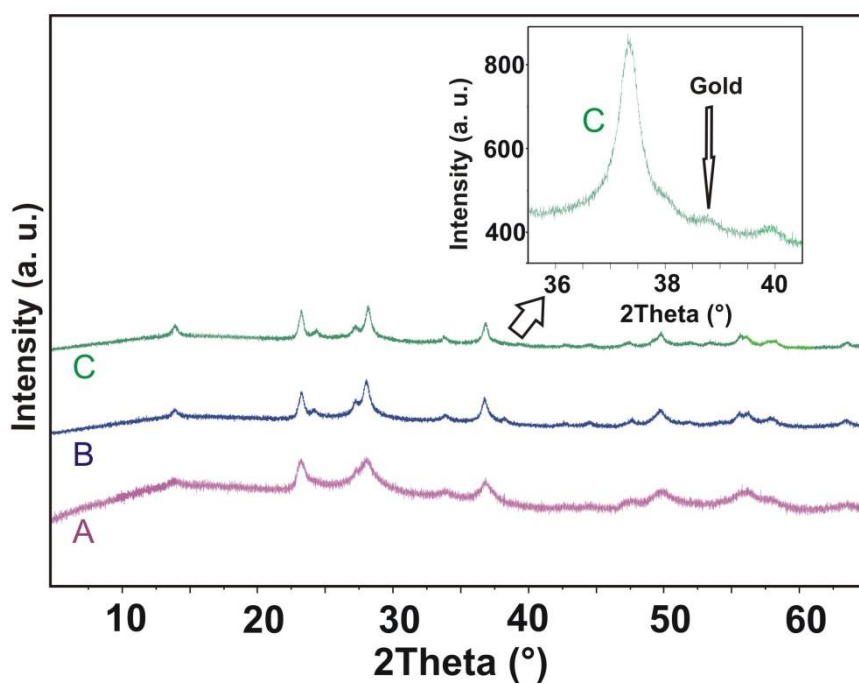
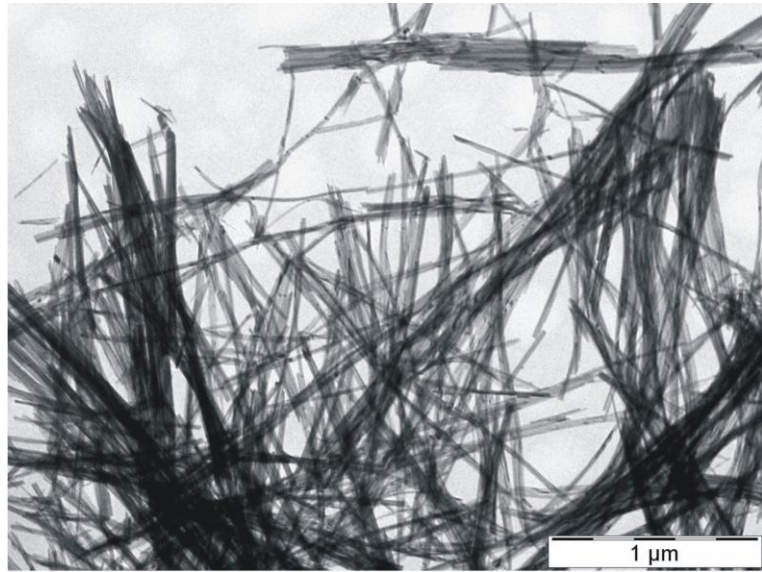
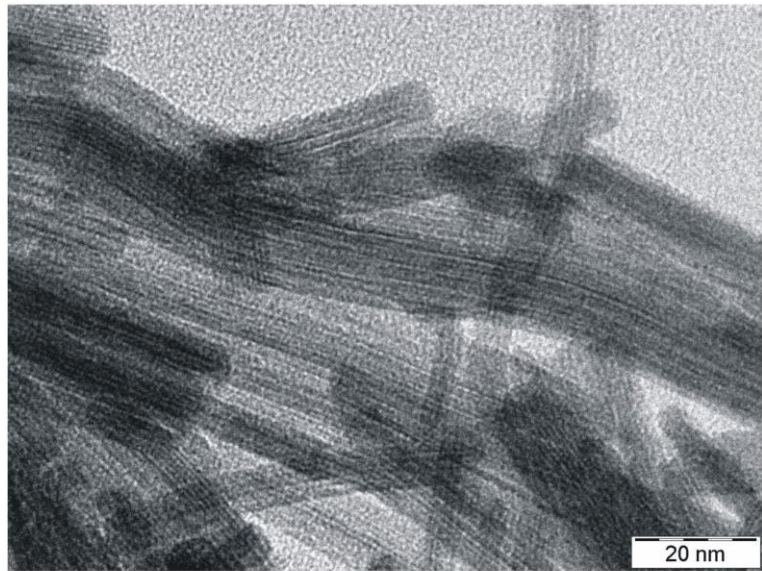


Figure 1.

**A**



**B**



**C**

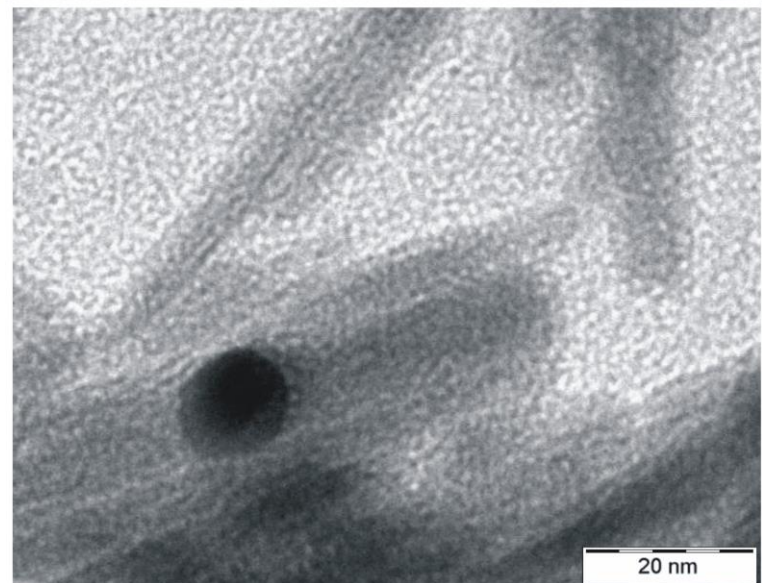


Figure 2.

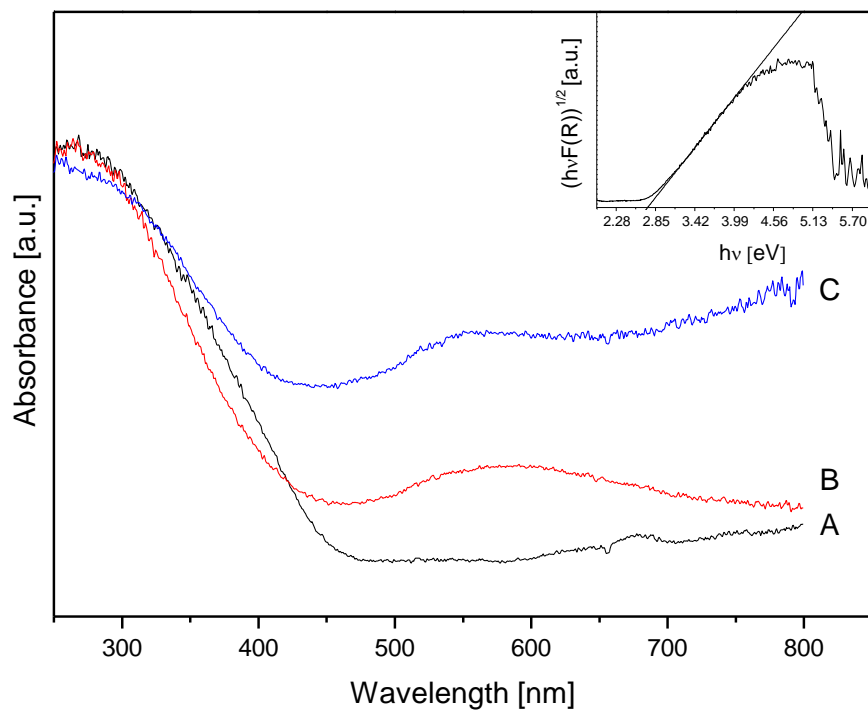


Figure 3.

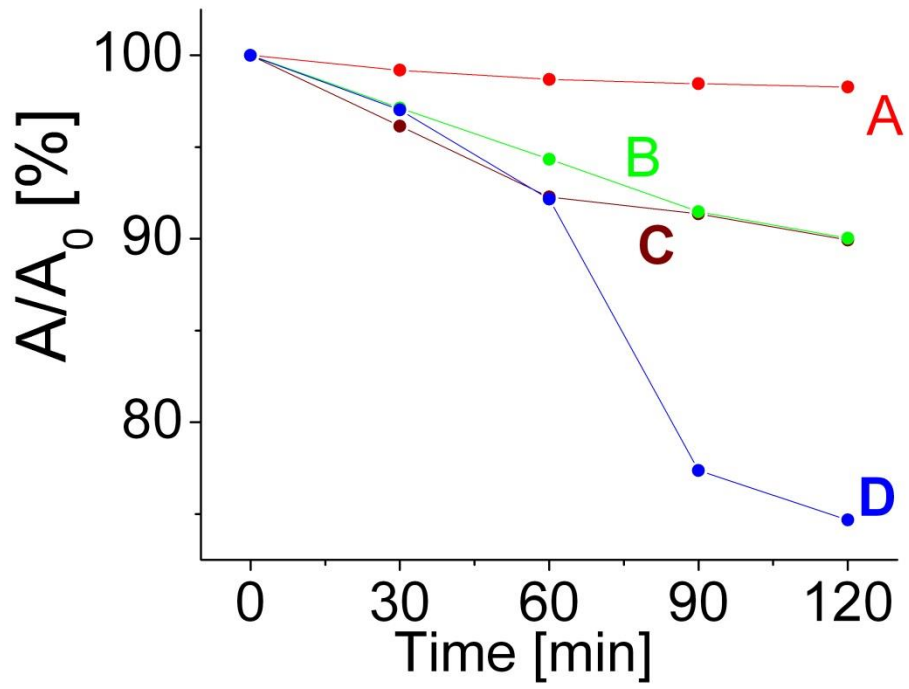


Figure 4.